Ag and Au atoms intercalated in bilayer heterostructures of transition metal dichalcogenides and graphene

F. Iyikanat, H. Sahin, R. T. Senger, and F. M. Peeters

Articles you may be interested in

Theory and synthesis of bilayer graphene intercalated with ICl and IBr for low power device applications
J. Appl. Phys. 114, 063702 (2013); 10.1063/1.4817498

Tunable electron and hole doping in FeCl3 intercalated graphene
Appl. Phys. Lett. 100, 213112 (2012); 10.1063/1.4722817

Electronic structures of an epitaxial graphene monolayer on SiC(0001) after metal intercalation (metal=Al, Ag, Au, Pt, and Pd): A first-principles study
Appl. Phys. Lett. 100, 063115 (2012); 10.1063/1.3682303

Trapping of metal atoms in the defects on graphene
J. Chem. Phys. 135, 224704 (2011); 10.1063/1.3666849

Fabrication of Li-intercalated bilayer graphene
AIP Advances 1, 022103 (2011); 10.1063/1.3582814

Ag and Au atoms intercalated in bilayer heterostructures of transition metal dichalcogenides and graphene

F. Iyikanat,[1,a] H. Sahin,[2,b] R. T. Senger,[1] and F. M. Peeters[2]
[1]*Department of Physics, Izmir Institute of Technology, 35430 Izmir, Turkey*
[2]*Department of Physics, University of Antwerp, 2610 Antwerp, Belgium*

The diffusive motion of metal nanoparticles Au and Ag on monolayer and between bilayer heterostructures of transition metal dichalcogenides and graphene are investigated in the framework of density functional theory. We found that the minimum energy barriers for diffusion and the possibility of cluster formation depend strongly on both the type of nanoparticle and the type of monolayers and bilayers. Moreover, the tendency to form clusters of Ag and Au can be tuned by creating various bilayers. Tunability of the diffusion characteristics of adatoms in van der Waals heterostructures holds promise for controllable growth of nanostructures. *© 2014 Author(s). All article content, except where otherwise noted, is licensed under a Creative Commons Attribution 3.0 Unported License.* [http://dx.doi.org/10.1063/1.4893543]

In recent years graphene[1] has become one of the most attractive materials due to its unique properties such as high-mobility electron transport,[2,3] the presence of room-temperature quantum Hall effect,[4] the strong lattice structure,[5] and the extremely high in-plane thermal conductivity.[6] However, its highly active surface and the lack of a band gap in the electronic structure are emerging drawbacks for graphene. Recently, interests have now also focused on other two-dimensional systems having honeycomb structures, such as graphane,[7,8] halogenated graphenes,[9–12] silicene,[13] III-V binary compounds,[14] and transition metal dichalcogenides (TMDs).[15–18] Recent studies have revealed that among various monolayer structures especially TMDs are quite promising materials for electronics and optoelectronics applications.

Bulk TMDs have a number of exceptional properties such as superconductivity of TaS_2 and $NbSe_2$, Mott transition in $1T\text{-}TaS_2$ and the presence of charge density wave in $TiSe_2$.[19,20] It was also reported that the electrical and optical properties of TMDs are dramatically altered with the number of layers.[21–23] Although bulk hexagonal TMDs possess an indirect bandgap, mono-layer TMDs exhibit a direct bandgap which is crucial for optoelectronic devices, sensors, and catalysts. In addition, n-type and p-type field-effect-transistors (FETs) based on monolayer and multilayer TMDs have been investigated.[24–26] It was also reported that many monolayer 2D crystals are reactive and segregation may occur easily.[27] Therefore, the investigation of bilayer structures which are chemically more stable than monolayer structures is of vital significance. Recent studies have shown that synthesis of heterostructures made of combinations of different TMD single layers, graphene, fluorographene, and hexagonal-BN (hBN) is experimentally achievable.[28–33] Since TMDs and other two-dimensional structures have a lot of diverse monolayer structures, when they are combined together they are expected to exhibit very different properties.[34,35]

Since the intercalation and migration of foreign atoms is inevitable during the formation of such lamellar materials and heterostructures, the investigation of the diffusion characteristics of various impurities is essential. Early studies revealed that alkali-metal doping of bulk $TiSe_2$ and MoS_2 can be utilized as an efficient way to tune the Fermi level.[36,37] The electrical conductivity of MoS_2 can be altered by substitutional doping.[38,39] Furthermore, decoration of the surfaces of few layer TMDs by

---

[a]Electronic mail: fadiliyikanat@iyte.edu.tr
[b]Electronic mail: hasan.sahin@uantwerpen.be

     2, 092801-1

metal nanoparticles such as Au, Ag, and Pt may provide p- and n-type doping.[40–43] The metal-atom adsorbed TMDs find their application in various areas including energy storage,[44] photonics,[45, 46] biosensing,[47] and catalysis.[48] In a recent study, it has been demonstrated that, the presence of various impurities at the interface between MoS_2/graphene/hBN and WS_2/graphene/hBN heterostructures may modify the mobility of charge carriers.[49] It was also reported that contamination and migration of various molecules are inevitable during the formation of graphene based heterostructures and trapped hydrocarbons segregate into isolated pockets, leaving the rest of the interface atomically clean.[50] In addition, it was found that, attached metal nanoparticles on TMDs/graphene stacks can be suitable for enhanced optoelectronic properties.[51, 52]

Despite some recent studies on adatom adsorption on various TMDs, intercalation and migration of foreign atoms in heterostructures have not been investigated. In this study, using density functional theory based electronic structure method, we investigate the diffusion characteristics of heavy metal atoms (Au and Ag) on monolayers and intercalated in such bilayer heterostructures. The paper is organized as follows: In "Computational methodology" we give our computational details. In "Diffusion of heavy atoms on monolayers of TMDs and graphene," the energetics of the metal atoms Ag and Au on monolayers of graphene and TMDs are presented. In "Diffusion of heavy atoms intercalated between van der Waals bilayers" we show the diffusion characteristics of those metal atoms inside bilayer heterostructures and in "Conclusion" we summarize and conclude our results.

Computational methodology: To determine ground state atomic structures and migration characteristics of monolayers and their bilayer heterostructures, first-principles calculations were performed using density functional theory (DFT) with a plane-wave basis set as implemented in the Vienna *ab initio* simulation package (VASP).[53] For the exchange correlation function generalized gradient approximation (GGA) of Perdew, Burke and Ernzerhof[54] was used together with the van der Waals correction.[55] Spin-unpolarized calculations were carried out using projector-augmented-wave potentials (PAW). The plane-wave basis set with kinetic energy cutoff of 500 eV was used.

A 4 × 4 and 3 × 3 hexagonal supercells of single layer and bilayer structures are employed to model diffusion paths of metal atoms, respectively. The k-point samples were 3 × 3 × 1 for these supercells. It is calculated that a 12 Å of vacuum space is enough to hinder long-range dispersion forces between two adjacent images in the supercell. Lattice constants and total energies were computed with the conjugate gradient method, where atomic forces and total energies were minimized. The convergence criterion of our calculations for ionic relaxations is 10^{-5} eV between two consecutive steps. The maximum Hellmann-Feynman forces acting on each atom were reduced to a value of less than 10^{-4} eV/Å. All components of the external pressure in the unit cell was held below 1 kbar. For the electronic density of states Gaussian smearing was used with a broadening of 0.1 eV. The non-local correlation energies were determined by employing density functional theory plus the long-range dispersion correction (DFT+D2) method.[55] The values of 24.670, 5.570, 12.640, 1.750, 24.670, 40.620, and 40.620 are used as the C_6 coefficient of Mo, S, Se, C, Ag, Au, and W atoms, respectively. On the other hand, values of 1.639, 1.683, 1.771, 1.452, 1.639, 1.772, and 1.772 are used for the vdW radius of Mo, S, Se, C, Ag, Au, and W atoms, respectively. These C_6 coefficients and vdW radii were determined from previous studies.[55, 56] It is essential that long-range dispersion correction to the interlayer force is taken into account in order to obtain reliable layer-layer distances and electronic properties of the heterobilayers.

To study the adsorption and diffusion of metal atoms in these systems, total energies of monolayer TMDs (graphene) with adatom were calculated for 19 (12) different points which include the high symmetry points (H, M, B, and T). Total energies of bilayers with adatom were calculated for only 4 high symmetry points. In these different points, the adatom-surface distance was fully relaxed while the position of the adatoms parallel to the surface was kept fixed. To obtain accurate diffusion characteristics of heavy atoms on monolayer TMDs and graphene, calculations were performed using 4 × 4 supercells. In these calculations, first and second nearest neighbors of the adatom were fully relaxed while all the rest was kept fixed. On the other hand, in the bilayer calculations, all atoms of bilayers were free to move in all directions. Binding energies were calculated for the most favorable adsorption sites. These binding energies were calculated from the expression $E_B = E_{Monolayer} + E_A - E_{Monolayer + A}$, where E_B is the binding energy of the metal atoms on the TMDs
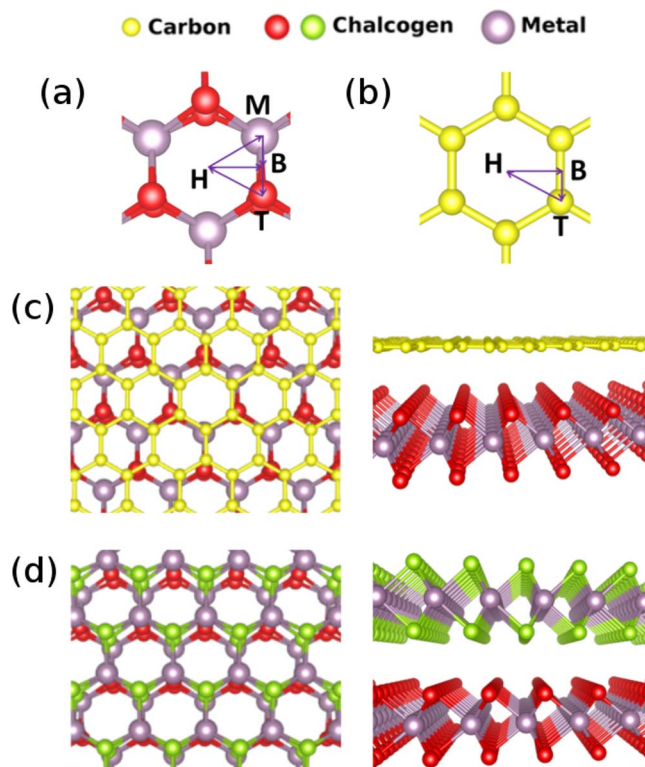
FIG. 1. Possible adsorption sites on (a) TMD and (b) Graphene. Top (left) and side (right) views of bilayer heterostructures of (c) TMD/Graphene and (d) TMD/TMD.

or graphene, $E_{Monolayer}$ is the energy of monolayer TMDs or graphene, E_A is the energy of metal atoms, $E_{Monolayer+A}$ is the total energy of the metal atom-monolayer system.

We have chosen the following convention to define the diffusion energy barrier. The binding energy of an adatom was calculated at all high-symmetry points of the TMDs and the graphene surface. Since adatoms follow the lowest energy path, the difference of the energies between the most favorable site and the second most favorable site was considered as the diffusion energy barrier.

In order to obtain the correct value of the charge transferred between the metal atoms, the TMDs and the graphene, Bader charge analysis was performed. Rather than electronic orbitals in Bader methodology, charge partitioning is based on electronic charge density and therefore it is highly efficient, it scales linearly with the number of grid points, and is more robust than other partitioning schemes.[57–59]

Diffusion of heavy atoms on monolayers of TMDs and graphene: So far, experiments have revealed that similar to graphene many of the TMDs (MoS_2, $MoSe_2$, WS_2, WSe_2, ReS_2) have a lamellar crystal structure where the layers are held together by weak van der Waals forces, while intra-layer metal-chalcogen bonds have strong covalent character. Due to the weakly (vdW) bonded layered structure of graphene and TMDs either diffusion of foreign atoms on their surface or easy intercalation into the layers may take place. Moreover, these foreign atoms may provide new functionalities to the TMDs and to the heterostructures made of various layered materials. Therefore, understanding how foreign atoms adsorb, migrate and intercalate are of highly importance.

First, we calculate the binding and migration of Ag and Au atoms on the surface of monolayer TMDs and graphene. For a hexagonal primitive unitcell of MoS_2, $MoSe_2$, WS_2, and graphene the lattice parameters are calculated to be 3.190, 3.316, 3.179, and 2.468 Å, respectively. For calculations of adsorption and migration of metal atoms 4 × 4 supercells, were used in order to limit Au-Au (and Ag-Ag) interaction between adjacent cells. As shown in Fig. 1 for a metal atom adsorbed on TMDs and graphene, there are four possible adsorption sites: top of carbon or chalcogen atom (T), bridge

TABLE I.   Several adsorption characteristics of adatoms on monolayer substrates. Binding site and $\Delta\rho$ denote the energetically most favorable position and change in the charge of adatom, respectively. Binding energy, height (relative to surface), energy barrier (at high symmetry sites, relative to the binding site), and jump probability (P) of the most favorable sites of Au and Ag atoms on the TMDs and graphene surface are listed.

	Ag/MoS$_2$	Ag/MoSe$_2$	Ag/WS$_2$	Ag/Graphene
Binding site	H	H	H	B
Binding energy (eV)	0.943	0.928	0.845	0.360
Height (Å)	1.97	2.07	2.04	2.57
$\Delta\rho = \rho_f - \rho_i$ (e)	−0.30	−0.18	−0.23	−0.16
Energy barrier (meV)	53(M), 146(B), 228(T)	44(M), 139(B), 241(T)	68(M), 111(B), 181(T)	2(T), 57(H)
Jump probability (P)	0.129	0.182	0.072	0.926
	Au/MoS$_2$	Au/MoSe$_2$	Au/WS$_2$	Au/Graphene
Binding site	T	H	T	T
Binding energy (eV)	1.161	1.232	1.146	0.633
Height (Å)	2.26	2.03	2.27	2.56
$\Delta\rho = \rho_f - \rho_i$ (e)	0.01	0.08	0.06	0.22
Energy barrier (meV)	136(M), 23(H), 46(B)	103(M), 72(B), 68(T)	180(M), 43(H), 55(B)	65(H), 26(B)
Jump probability (P)	0.411	0.072	0.189	0.366

site on C-C or M-X bond (B), on top of the center of hollow site (H), and on top of metal atom Mo or W (M).

Diffusion and mobility of impurities on a two-dimensional crystal surface can be described by quantities such as activation energy (E_a) and jump probability (P) from the binding site over the lowest-barrier path at room temperature. The P value is a measure of the possibility of propagation by overcoming the energy barrier among the possible adsorption sites. Jump probability from one lattice site to another one can be calculated by using the formula $P \approx e^{-E_a/k_B T}$ where k_B is the Boltzmann constant and it increases exponentially with increasing temperature. Here E_a is the activation energy which is equal to the difference of the energy of the two lowest energy states.

Our calculated adsorption sites, binding energies, vertical adsorption position, charge transfer, energy barrier, and jump probability (P) values are listed in Table I. We see that the bonding of an Ag atom to graphene occurs at the B site and the H site is the least favorable adsorption site. In accordance with the previous DFT study, we found that the binding energy of Au on graphene is almost twice the binding energy of Ag on graphene. The Ag atoms lose (while the Au atoms gain) a small amount of charge when they bind to the graphene surface.[60] On the surface of TMDs, the most favorable bonding site for Ag atoms is the H site and the next largest adsorption energy is found for the M site. It is reasonable to assume that metal atoms diffuse through these two favorable adsorption sites. Therefore, the energy difference between these two lowest-energy sites can be regarded as the diffusion barrier. Since the energy barrier for Ag between H and M sites is high (∼50 meV) diffusion through these symmetry points may not occur at low temperatures. It appears from Fig. 2 that Ag atoms on graphene migrate through the B and T sites with almost zero (∼2 meV) energy barrier, while migration on TMDs (MoS$_2$, MoSe$_2$, and WS$_2$) occurs through H and M sites. As shown in Table I, room temperature P values of Ag atoms are 0.129, 0.182, 0.072, and 0.926 for MoS$_2$, MoSe$_2$, WS$_2$, and graphene, respectively. Thus diffusion of the Ag atoms on graphene occurs much more easily than on TMDs.

Binding energy of a single Au atom on graphene and TMDs is found to be ∼300 meV larger than that of Ag. Interestingly, on MoSe$_2$, Au atoms prefer bonding on the H site like Ag atoms, while the top of a sulfur atom (T site) is the most preferable site on MoS$_2$ and WS$_2$ layers. The distinctive behavior of the Au atoms can be explained by the distinctive characteristic of the S-Au bond. Although the chemical properties of chalcogen atoms S and Se are quite similar, as shown by Yee *et al.*,[61] the strength of the S-Au bond is slightly weaker than the Se-Au bond. Our calculations reveal that the binding energy of an Au atom on MoSe$_2$ surface is higher than the binding energy of an Au atom on MoS$_2$ and WS$_2$ surfaces. Interestingly, strong Au-S bonds require bonding on T
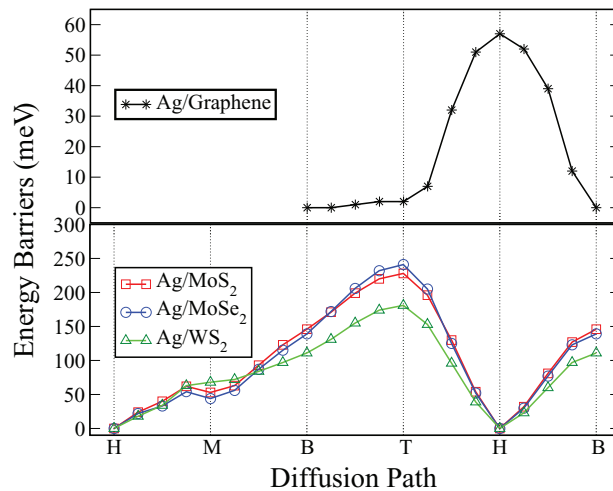
FIG. 2. Diffusion paths of Ag on Graphene, MoS_2, $MoSe_2$, and WS_2. (see Fig. 1 for sites.)
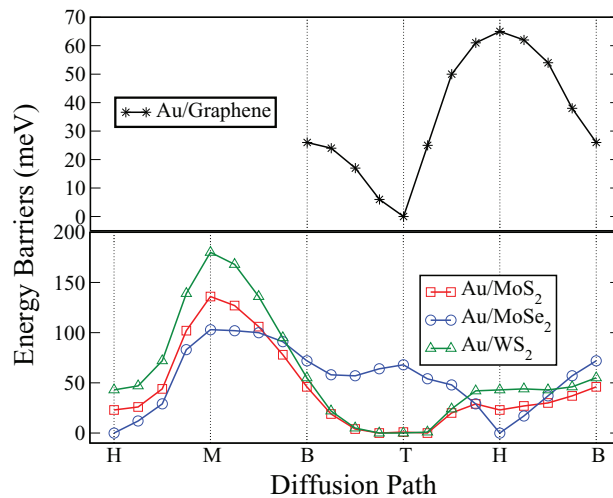
FIG. 3. Diffusion paths of Au on Graphene, MoS_2, $MoSe_2$, and WS_2. (see Fig. 1 for sites.)

site while the Au-Se bond results in H-site adsorption. As shown in Fig. 3, as in the Ag adsorption case, MoS_2 and WS_2 surfaces have almost identical characteristics for Au adsorption at all high symmetry points. In addition, the migration barrier seen by Au atoms is ∼30 meV larger than the energy barrier of Ag atoms on graphene. Therefore, compared to Ag on graphene, the smaller jump probability of Au atoms on graphene implies relatively slow and smaller nucleation of Au clusters on graphene which agrees with experimental results.[62]

Calculated room temperature P values of an Au atom on MoS_2, $MoSe_2$, WS_2, and graphene surfaces are 0.411, 0.072, 0.189, and 0.366, respectively. Au atom has the maximum P value on a MoS_2 surface, whereas it has the minimum P value on a $MoSe_2$ surface. P values of Au atoms on a MoS_2 surface is higher than that of Ag atoms. This result is consistent with the previous experimental study where they found that the cluster diameter of Au and Ag atoms on MoS_2 were found to be 14 and 6 nm, respectively.[63] Other experimental work showed that cluster diameters of Au and Ag atoms on WS_2 are 19-20 and 5 nm, respectively.[44] In agreement with this experimental study, our calculations show that the P value of the Au atoms on a WS_2 surface is higher than that of Ag atoms.

Diffusion of heavy atoms intercalated between van der Waals bilayers: The vertical stacking of graphene and other two-dimensional atomic crystals allows for the combination of different electronic properties. Recent studies have shown that, electronic and optical properties of TMDs

TABLE II. Several adsorption characteristic of adatoms between bilayer heterostructures. Binding site and $\Delta\rho$ denotes the energetically most favorable position and change in the charge of adatom, respectively. LL distance gives the interlayer distance. Intercalation energy, height above MoS_2, energy barrier (at high symmetry sites, relative to the binding site), and jump probability (P) of the most favorable sites of Au and Ag atoms between bilayer heterostructures are listed.

	$MoS_2/Ag/MoS_2$	$MoS_2/Ag/MoSe_2$	$MoS_2/Ag/WS_2$	$MoS_2/Ag/Graphene$
Binding site	H	H	H	M
Intercalation energy (eV)	−1.461	−1.395	−1.319	−1.344
Height above MoS_2 (Å)	1.85	1.71	1.85	1.61
$\Delta\rho = \rho_f - \rho_i$ (e)	−0.42	−0.41	−0.41	−0.47
LL distance (pristine, with Ag)	3.08, 3.70	3.10, 3.60	3.09, 3.71	3.32, 3.86
Energy barrier (meV)	222(M), 282(B), 222(T)	206(M), 308(B), 274(T)	243(M), 295(B), 340(T)	43(H), 196(T)
Jump probability (P)	2×10^{-4}	3.5×10^{-4}	8×10^{-5}	0.189
	$MoS_2/Au/MoS_2$	$MoS_2/Au/MoSe_2$	$MoS_2/Au/WS_2$	$MoS_2/Au/Graphene$
Binding site	B	H	H	T
Intercalation energy (eV)	−1.645	−1.562	−1.504	−1.541
Height above MoS_2 (Å)	2.07	1.79	1.85	2.07
$\Delta\rho = \rho_f - \rho_i$ (e)	−0.15	−0.13	−0.18	−0.21
LL distance (pristine, with Au)	3.08, 4.12	3.10, 3.72	3.09, 3.74	3.32, 4.35
Energy barrier (meV)	12(H), 96(M), 95(T)	118(M), 75(B), 103(T)	78(M), 24(B), 164(T)	468(H) 326(M)
Jump probability (P)	0.628	0.055	0.395	3×10^{-6}

can be altered dramatically by forming such heterostructures.[28,64] It appears that the intercalation and contamination of foreign atoms and functional groups at the interface of these heterostructures are unavoidable. As shown by recent experimental study, heavy atoms such as Au and Ag are quite mobile on TMD surfaces and they form clusters.[65] Therefore, understanding the diffusion characteristics of heavy atoms at the interface of these heterostructures is of importance for the ongoing research on heterostructure devices.

In this section, we investigate the diffusion characteristics of Au and Ag atoms intercalated in $MoS_2/Graphene$, MoS_2/MoS_2, $MoS_2/MoSe_2$, and MoS_2/WS_2 heterostructures.

(a) Diffusion through MoS_2/graphene bilayer heterostructure: First, we start with the heterostructure $MoS_2/Graphene$. However, the determination of the most favorable atomic structure of $MoS_2/Graphene$ heterostructure is more complicated due to the lattice mismatch. Our calculations showed that bare DFT calculations are not capable of finding the ground state ordering of graphene placed on MoS_2 due to the presence of many local minima corresponding to metastable states. It was seen that low-temperature (100 K) molecular dynamic calculations are able to avoid local minima allowing to obtain the relaxed geometric structure of $MoS_2/Graphene$ as shown in Fig. 1(c). Due to the lack of symmetry in the $MoS_2/Graphene$ structure, 27 inequivalent adsorption sites are considered for each Ag (and Au) atom adsorption. Table II lists the intercalation energies obtained by using a 3×3 unit cell of the most favorable site for each configuration. Here the intercalation energy is defined by the expression

$$E_{int} = E_{Hetero+Ag(Au)} - E_{Hetero} - E_{Ag(Au)}, \tag{1}$$

where E_{int} is the intercalation energy of Ag(Au) atom, $E_{Hetero + Ag(Au)}$ is the energy of the metal-atom heterobilayer system, E_{Hetero} is the energy of heterobilayers, and $E_{Ag(Au)}$ is the energy of the adatom. Due to the large binding energies of adatoms on MoS_2, all the equilibrium geometries are ruled by MoS_2 except for the $MoS_2/Au/MoSe_2$ structure where Au's binding is larger with the $MoSe_2$ layer.

Our calculations revealed that binding energies of Ag and Au atoms on TMD substrates are larger than that on graphene and Au atoms are more stable than Ag atoms on these monolayers. For the simulation of the $MoS_2/Graphene$ heterostructure we considered 4×4 and 3×3 unit cells for graphene and MoS_2 layers, respectively. After full optimization, the lattice parameter of the heterostructure is calculated to be 9.791 Å. For this supercell the maximum lattice mismatch is ∼3%.
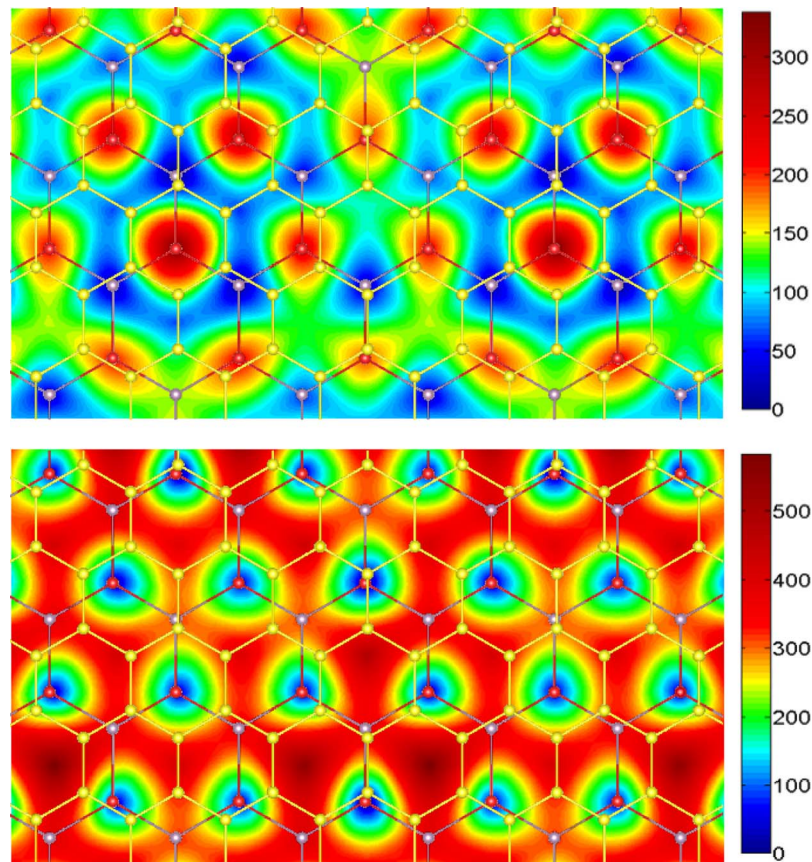
FIG. 4. Contour plots of the energy barriers (in meV units) seen by Ag (upper panel) and Au (lower panel) atoms intercalated in MoS_2/Graphene heterostructure.

The adsorption energies and the equilibrium geometries were calculated by considering 27 different adsorption sites for each Ag and Au atoms at the MoS_2/Graphene interface. It is seen that the most favorable site of Ag atoms on MoS_2 is changed from H to M site upon the addition of the graphene layer. Energy barrier of Ag atoms is enhanced from 2 to 43 meV with graphene layer. Although the energy barriers seen by Au atom on MoS_2 are significantly enhanced by the presence of the graphene layer, the T site of MoS_2 remains as the most favorable adsorption site of Au.

Furthermore, we show 2D plots of the energy barriers seen by Ag and Au atoms at the MoS_2/Graphene interface in Fig. 4. It is clear that Ag and Au atoms have entirely different diffusion characteristics at the MoS_2/Graphene interface: (i) diffusion of Ag atoms are much easier while Au atoms may diffuse at high temperatures, (ii) diffusion of an Ag atom occurs through the bridge sites of the top-lying graphene layer, (iii) diffusion of Au atom may occur from one top-sulfur site to another one through the top site of Mo atoms. Here, similar characteristic diffusion behavior of heavy atoms can be expected for bilayer heterostructures of WS_2/Graphene as well.

(b) *Diffusion through MX_2/MX_2 bilayer heterostructures:* Next, we investigate the diffusion and energy barriers which are seen by Ag and Au atoms sandwiched in between single layers of TMDs. There are two possible stacking types for bilayer TMDs; AA and AB stacking. In the AA stacking, the chalcogen atom (S or Se) in one layer is on top of the chalcogen atom (S or Se) of the other layer. On the other hand, in AB stacking, chalcogen atom (S or Se) in one layer is on top of the metal atoms (Mo or W) of the other layer. Our calculations show that for the considered bilayer heterostructures of TMDs, the AB stacking is the ground state geometry.

MoS_2/MoS_2 bilayers: The lattice parameter of AB-stacked bilayer MoS_2/MoS_2 structure was found to be almost the same as of monolayer MoS_2. It is seen that the Ag-MoS_2 distance decreases

due to the presence of the upper MoS_2 layer. The layer-layer distance of bilayer MoS_2 increases from 3.08 to 3.70 Å upon single Ag intercalation. On the other hand, single Au atom causes a larger layer separation (from 3.08 to 4.12 Å) than Ag atoms. Our calculations revealed that the most preferable site of the Ag atom remains the H-site, even after the addition of the second layer. Our charge analysis showed that metal atoms tend to donate a larger amount of charge when they are intercalated in bilayers. The amount of charge transfer becomes $0.42e$ and $0.15e$ for Ag and Au atoms, respectively. However, it is worthwhile to note that the preferable adsorption site for Au atoms changes from T to B site. Au atoms tend to bind with two S atoms that are in two different layers. For this reason, the B-site is the most favorable site.

The minimum diffusion barrier of Ag atom is increased by $\sim$170 meV after the addition of the second layer. Interestingly diffusion barriers of the Ag atom between bilayer MoS_2 from H to M and H to T sites are the same. The minimum diffusion barrier of Au atom is reduced by half when a second layer is added. These results show that the diffusion behavior of Ag and Au atoms between bilayer MoS_2 are completely different. Ag atoms are not likely to form clusters inside the bilayer MoS_2. On the other hand, Au atoms may form clusters between two MoS_2 layers and the clusterization weight of them is larger than that on single layer of MoS_2.

MoS_2/$MoSe_2$ bilayers: For the geometry optimization of the MoS_2/$MoSe_2$ bilayer structure we performed full atomic and lattice parameter relaxation and therefore internal strain due to lattice mismatch is lowered to less than 1 kB. The lattice parameter of MoS_2/$MoSe_2$ is calculated to be 3.252 Å. For this lattice parameter, the maximum lattice mismatch is $\sim$2% which is in the range of experimentally available strain values. When Au and Ag atoms are intercalated between MoS_2/$MoSe_2$, they show the same trend; their height above the MoS_2 surface are fairly close (1.7 Å for Ag and 1.8 Å for Au) and the layer-layer distance increases from 3.1 to 3.6 and 3.7 Å for Ag and Au, respectively. H-site is the most favorable site for Ag and Au atoms when they are located between MoS_2/$MoSe_2$ bilayer. When Ag atom is inserted in MoS_2/$MoSe_2$, it donates $0.41e$ to neighboring TMD layers. It appears that the majority of the charges are transferred to the MoS_2 layer. Similarly, the Au atom loses $0.13e$ charge when inserted between MoS_2/$MoSe_2$. The minimum diffusion barrier of Ag atom is increased by $\sim$150 meV when the second layer is present. But the second favorable site does not change with the addition of the $MoSe_2$ layer (M). The minimum diffusion barrier of Au atom increases from 23 to 75 meV with $MoSe_2$ addition. Second favorable site of Au atom changes from H to B site when $MoSe_2$ layer is added. Similar to MoS_2/MoS_2, the jump probability of Ag atom becomes zero with the addition of $MoSe_2$ as a second layer. The P value of Au atom decreases from 0.411 to 0.055 with the addition of $MoSe_2$ layer. Therefore, the formation of Ag cluster between MoS_2/$MoSe_2$ bilayer heterostructure is hindered by the presence of the second layer. The nucleation of Au clusters may happen with a slower nucleation rate in MoS_2/$MoSe_2$ as compared to monolayer MoS_2.

MoS_2/WS_2 bilayers: The lattice mismatch between MoS_2 and WS_2 is negligible and the lattice parameter of the bilayer structure was calculated to be 3.182 Å. Both Au and Ag atoms prefer to be bonded on the H site 1.85 Å away from the surface of MoS_2. When Ag and Au atoms are inserted between MoS_2/WS_2, the interlayer distances increase from 3.09 to 3.71 and 3.74 Å, respectively. We found that the Ag atom donates $0.41e$ to the surrounding MoS_2/WS_2 bilayer structure whereas the amount of charge transfer is $0.18e$ for Au. The minimum diffusion barrier of the Ag atom increases $\sim$190 meV with the addition of WS_2 layer, but it does not change the second favorable site of Ag atom (M). It is seen that the addition of the WS_2 layer does not have any significant effect on the minimum diffusion barrier of the Au atom.

In this case, the change of the P value of the Ag atom shows the same trend with bilayer MoS_2 and MoS_2/$MoSe_2$. In these cases, the P value of Ag atom becomes zero with the addition of the second layer (WS_2 in this case). On the other hand, addition of a WS_2 layer does not change the P value of the Au atom between MoS_2/WS_2, significantly. As a result, Ag atoms are not likely to form clusters when intercalated in MoS_2/WS_2, while the clusterization probability of Au atoms does almost not change with WS_2 layer addition.

Conclusion: We found that the binding energy of Ag and Au atoms is maximum when they are placed on MoS_2 and $MoSe_2$, respectively, and the binding energy of these atoms on graphene is lower than that on TMDs. Ag atoms prefer to bind at the H site on TMDs, while the H and the

T sites are most favorable adsorption sites for Au atoms. Just as for the Ag atom, Au atom binds to H site on $MoSe_2$. However, Au atom binds to T site on MoS_2 and WS_2. When Ag atom adsorbs on these monolayers, it tends to donate charge, whereas Au atom tends to receive charge from these monolayers. Calculated *P* values revealed that, clusterization tendency of Ag and Au are the largest on graphene and MoS_2 layers, respectively.

Addition of a second layer has a considerable effect on the diffusion phenomena of Ag and Au atoms. Ag atom binds to H site of all TMDs heterostructures, whereas it binds to M site of the MoS_2/Graphene heterostructure. When an Au atom is inserted between MoS_2/$MoSe_2$ and MoS_2/WS_2 heterostructures, H site is the energetically most favorable site. B and T sites are the most favorable sites for the Au atom when it is placed between MoS_2/MoS_2 and MoS_2/Graphene heterostructures. The clusterization probability of Ag atom becomes zero when TMDs are added as a second layer. On the other hand, the *P* value of Ag atom increases with the addition of a graphene layer. Addition of a graphene layer hinders diffusion of Au atom. WS_2 addition as a second layer, does not make a significant effect on the cluster formation probability of Au atom. Addition of $MoSe_2$ as a second layer reduces the clusterization of Au, whereas the addition of a second MoS_2 layer increases it. Our calculated intercalation energies showed that, when Au and Ag atoms are inserted between MoS_2/Graphene, MoS_2/MoS_2, MoS_2/$MoSe_2$ or MoS_2/WS_2, they are energetically more stable as compared to the case where Ag and Au atoms are adsorbed on the monolayer substrates. The energy barrier for Au atoms is lower than the one for Ag atoms, when they are inserted between TMD heterostructures. On the other hand, the energy barrier of Ag atoms is lower than the energy barrier of Au atoms when they are inserted between MoS_2/Graphene. Tunability of diffusion barriers seen by adatoms in van der Waals heterostructures makes these materials potential hosts for controlled growth of nanoclusters.

[1] K. S. Novoselov, A. K. Geim, S. V. Morozov, D. Jiang, Y. Zhang, S. V. Dubonos, I. V. Grigorieva, and A. A. Firsov, Science **306**, 666 (2004).

[2] K. S. Novoselov, A. K. Geim, S. V. Morozov, D. Jiang, M. I. Katsnelson, I. V. Grigorieva, S. V. Dubonos, and A. A. Firsov, Nature **438**, 197 (2005).

[3] K. I. Bolotin, K. J. Sikes, J. Hone, H. L. Stormer, and P. Kim, Phys. Rev. Lett. **101**, 096802 (2008).

[4] K. S. Novoselov, Z. Jiang, Y. Zhang, S. V. Morozov, H. L. Stormer, U. Zeitler, J. C. Maan, G. S. Boebinger, P. Kim, and A. K. Geim, Science **315**, 1379 (2007).

[5] C. Lee, X. Wei, J. W. Kysar, and J. Hone, Science **321**, 385 (2008).

[6] J. H. Seol, I. Jo, A. L. Moore, L. Lindsay, Z. H. Aitken, M. T. Pettes, X. Li, Z. Yao, R. Huang, D. Broido, N. Mingo, R. S. Ruoff, and L. Shi, Science **328**, 213 (2010).

[7] J. O. Sofo, A. S. Chaudhari, and G. D. Barber, Phys. Rev. B **75**, 153401 (2007).

[8] M. Z. S. Flores, P. A. S. Autreto, S. B. Legoas, and D. S. Galvao, Nanotechnology **20**, 465704 (2009).

[9] R. R. Nair, W. Ren, R. Jalil, I. Riaz, V. G. Kravets, L. Britnell, P. Blake, F. Schedin, A. S. Mayorov, S. Yuan, M. I. Katsnelson, H. M. Cheng, W. Strupinski, L. G. Bulusheva, A. V. Okotrub, I. V. Grigorieva, A. N. Grigorenko, K. S. Novoselov, and A. K. Geim, Small **6**, 2877 (2010).

[10] H. Sahin, M. Topsakal, and S. Ciraci, Phys. Rev. B **83**, 115432 (2011).

[11] H. Peelaers, A. D. Hernandez-Nieves, O. Leenaerts, B. Partoens, and F. M. Peeters, Appl. Phys. Lett. **98**, 051914 (2011).

[12] H. Sahin, and S. Ciraci, J. Phys. Chem. C **116**, 24075 (2012).

[13] A. Kara, H. Enriquez, A. P. Seitsonen, L. C. L. Y. Voon, S. Vizzini, B. Aufray, and H. Oughaddou, Surf. Sci. Rep. **67**, 1 (2012).

[14] H. Sahin, S. Cahangirov, M. Topsakal, E. Bekaroglu, E. Akturk, R. T. Senger, and S. Ciraci, Phys. Rev. B **80**, 155453 (2009).

[15] L. F. Mattheiss, Phys. Rev. B **8**, 3719 (1973).

[16] M. Chhowalla, H. S. Shin, G. Eda, L. J. Li, K. P. Loh, and H. Zhang, Nat. Chem. **5**, 263 (2013).

[17] Y. Ma, Y. Dai, M. Guo, C. Niu, Y. Zhu, and B. Huang, ACS Nano **6**(2), 1695 (2012).

[18] S. Tongay, H. Sahin, C. Ko, A. Luce, W. Fan, K. Liu, J. Zhou, Y. S. Huang, C. H. Ho, J. Yan, D. F. Ogletree, S. Aloni, J. Ji, S. Li, J. Li, F. M. Peeters, and J. Wu, Nat. Commun. **5**, 3252 (2014).

[19] B. Sipos, A. F. Kusmartseva, A. Akrap, H. Berger, L. Forro, and E. Tutis, Nat. Mater. **7**, 960 (2008).

[20] R. A. Jishi and H. M. Alyahyaei, Phys. Rev. B **78**, 144516 (2008).

[21] A. Splendiani, L. Sun, Y. Zhang, T. Li, J. Kim, C. Y. Chim, G. Galli, and F. Wang, Nano Lett. **10**, 1271 (2010).

[22] E. Cappelluti, R. Roldan, J. A. Silva-Guillen, P. Ordejon, and F. Guinea, Phys. Rev. B **88**, 075409 (2013).

[23] H. Sahin, S. Tongay, S. Horzum, W. Fan, J. Zhou, J. Li, J. Wu, and F. M. Peeters, Phys. Rev. B **87**, 165409 (2013).

[24] S. Das, H. Y. Chen, A. V. Penumatcha, and J. Appenzeller, Nano Lett. **13**, 100 (2013).

[25] B. Radisavljevic, A. Radenovic, J. Brivio, V. Giacometti, and A. Kis, Nat. Nanotechnol. **6**, 147 (2011).

[26] H. Fang, S. Chuang, T. C. Chang, K. Takei, T. Takahashi, and A. Javey, Nano Lett. **12**, 3788 (2012).

[27] A. K. Geim, Intern. J. Mod. Phys. B **25**, 4055 (2011).

[28] A. K. Geim, and I. V. Grigorieva, Nature **499**, 419 (2013).

[29] H. Terrones, F. López-Urías, and M. Terrones, Sci. Rep. **3**, 1549 (2013).

[30] M. S. Choi, G.-H. Lee, Y.-J. Yu, D.-Y. Lee, S. H. Lee, P. Kim, J. Hone, and W. J. Yoo, Nat. Commun. **4**, 1624 (2013).

[31] L. Britnell, R. V. Gorbachev, R. Jalil, B. D. Belle, F. Schedin, A. Mishchenko, T. Georgiou, M. I. Katsnelson, L. Eaves, S. V. Morozov, N. M. R. Peres, J. Leist, A. K. Geim, K. S. Novoselov, and L. A. Ponomarenko, Science **335**, 947 (2012).

[32] C. Dean, A. F. Young, L. Wang, I. Meric, G. H. Lee, K. Watanabe, T. Taniguchi, K. Shepard, P. Kim, and J. Hone, Solid State Commun. **152**, 1275 (2012).

[33] T. Georgiou, R. Jalil, B. D. Belle, L. Britnell, R. V. Gorbachev, S. V. Morozov, Y. J. Kim, A. Gholinia, S. J. Haigh, O. Makarovsky, L. Eaves, L. A. Ponomarenko, A. K. Geim, K. S. Novoselov, and A. Mishchenko, Nat. Nanotechnol. **8**, 100 (2012).

[34] Y. Ma, Y. Dai, W. Wei, C. Niu, L. Yu, and B. Huang, J. Phys. Chem. C **115**(41), 20237 (2011).

[35] X. Li, Y. Dai, Y. Ma, S. Han, and B. Huang, Phys. Chem. Chem. Phys. **16**, 4230 (2014).

[36] P. Joensen, R. F. Frindt, and S. R. Morrison, Mater. Res. Bull. **21**, 457 (1986).

[37] W. Jaegermann, C. H. Pettenkofer, A. Schellenberger, C. A. Papageorgopoulos, M. Kamaratos, D. Vlachos, and Y. Tomm, Chem. Phys. Lett. **221**, 441 (1994).

[38] K. K. Tiong, Y. S. Huang, and C. H. Ho, J. Alloys Compd. **317**, 208 (2001).

[39] V. V. Ivanovskaya, A. Zobelli, A. Gloter, N. Brun, V. Serin, and C. Colliex, Phys. Rev. B **78**, 134104 (2008).

[40] C. N. R. Rao, H. S. S. R. Matte, R. Voggu, and A. Govindaraj, Dalton Trans. **41**, 5089 (2012).

[41] Y. Shi, J. K. Huang, L. Jin, Y. T. Hsu, S. F. Yu, L. J. Li, and H. Y. Yang, Sci. Rep. **3**, 1839 (2013).

[42] J. Kim, S. Byun, A. J. Smith, J. Yu, and J. Huang, J. Phys. Chem. Lett. **4**, 1227 (2013).

[43] H. D. Ozaydin, H. Sahin, R. T. Senger, and F. M. Peeters, "Formation and diffusion characteristics of Pt clusters on graphene, 1H-MoS$_2$ and 1T-TaS$_2$," Ann. Phys. (published online).

[44] H. S. S. Matte, U. Maitra, P. Kumar, B. G. Rao, K. Pramoda, and C. N. R. Rao, Z. Anorg. Allg. Chem. **638**, 2617 (2012).

[45] F. Huang, and J. J. Baumberg, Nano Lett. **10**, 1787 (2010).

[46] H. Qian, Y. Zhu, and R. Jin, Proc. Natl. Acad. Sci. U. S. A. **109**, 696 (2012).

[47] S. He, K. K. Liu, S. Su, J. Yan, X. Mao, D. Wang, Y. He, L. J. Li, S. Song, and C. Fan, Anal. Chem. **84**, 4622 (2012).

[48] Y. C. Lu, Z. Xu, H. A. Gasteiger, S. Chen, K. Hamad-Schifferli, and Y. Shao-Horn, J. Am. Chem. Soc. **132**, 12170 (2010).

[49] A. V. Kretinin, Y. Cao, J. S. Tu, G. L. Yu, R. Jalil, K. S. Novoselov, S. J. Haigh, A. Gholinia, A. Mishchenko, M. Lozada, T. Georgiou, C. R. Woods, F. Withers, P. Blake, G. Eda, A. Wirsig, C. Hucho, K. Watanabe, T. Taniguchi, A. K. Geim, and R. V. Gorbachev, Nano Lett. **14**(6), 3270 (2014).

[50] S. J. Haigh, A. Gholinia, R. Jalil, S. Romani, L. Britnell, D. C. Elias, K. S. Novoselov, L. A. Ponomarenko, A. K. Geim, and R. Gorbachev, Nat. Mater. **11**, 764 (2012).

[51] L. Britnell, R. M. Ribeiro, A. Eckmann, R. Jalil, B. D. Belle, A. Mishchenko, Y. J. Kim, R. V. Gorbachev, T. Georgiou, S. V. Morozov, A. N. Grigorenko, A. K. Geim, C. Casiraghi, A. H. C. Neto, and K. S. Novoselov, Science **340**, 1311 (2013).

[52] B. Sachs, L. Britnell, T. O. Wehling, A. Eckmann, R. Jalil, B. D. Belle, A. I. Lichtenstein, M. I. Katsnelson, and K. S. Novoselov, Appl. Phys. Lett. **103**, 251607 (2013).

[53] G. Kresse and J. Furthmüller, Phys. Rev. B **54**, 11169 (1996).

[54] J. P. Perdew, K. Burke, and M. Ernzerhof, Phys. Rev. Lett. **77**, 3865 (1996).

[55] S. Grimme, J. Comput. Chem. **27**, 1787 (2006).

[56] M. Amft, S. Lebegue, O. Eriksson, and N. V. Skorodumova, J. Phys. **23**, 395001 (2011).

[57] G. Henkelman, A. Arnaldsson, and H. Jónsson, Comput. Mater. Sci. **36**, 354 (2006).

[58] W. Tang, E. Sanville, and G. Henkelman, J. Phys.: Condens. Mater. **21**, 084204 (2009).

[59] E. Sanville, S. D. Kenny, R. Smith, and G. Henkelman, J. Comput. Chem. **28**, 899 (2007).

[60] K. Nakada and A. Ishii, "DFT Calculation for Adatom Adsorption on Graphene," in *Nanotechnology and Nano-materials "Graphene Simulation*, edited by Jian Ru Gong (InTech, 2011), p. 978. See http://www.intechopen.com/books/graphene-simulation/dft-calculation-for-adatom-adsorption-on-graphene.

[61] C. K. Yee, A. Ulman, J. D. Ruiz, A. Parikh, H. White, and M. Rafailovich, Langmuir **19**, 9450 (1992).

[62] K. S. Subrahmanyam, A. K. Manna, and S. K. Pati, Chem. Phys. Lett. **497**, 70 (2010).

[63] B. G. Rao, H. S. S. R. Matte, and C. N. R. Rao, J. Cluster Sci. **23**(3), 929 (2012).

[64] H. P. Komsa and A. V. Krasheninnikov, Phys. Rev. B **88**, 085318 (2013).

[65] C. Gong, C. Huang, J. Miller, L. Cheng, Y. Hao, D. Cobden, J. Kim, R. S. Ruoff, R. M. Wallace, K. Cho, X. Xu, and Y. J. Chabal, ACS Nano **7**, 11350 (2013).